An Isotopic Study of Glauconite from Lower Ordovician Limestone, Stenbröttet, Sweden

by

Tom Eggert

The Ohio State University

1979

Fall Quarter

Gunter Faure

Gunter Faure

Advisor

TABLE OF CONTENTS

ABSTRACT

Glauconites separated from Lower Ordovician limestones collected near Stenbröttet, southern Sweden, were dated by the Rb-Sr method. Strontium and rubidium concentrations in the samples were determined by X-ray fluorescence analysis. Strontium isotope ratios were determined by isotope analysis of strontium on a mass spectrometer. Rb-Sr model dates were calculated with data so obtained and by use of the following equation derived from the law of radioactivity:

$$t = \frac{\ln}{\lambda}\left[\frac{^{87}Sr/^{86}Sr - (^{87}Sr/^{86}Sr)_o}{^{87}Rb/^{86}Sr} + 1\right],$$

where t is a date in the geologic past and λ is the decay constant for the decay of ^{87}Rb to ^{87}Sr. Calculated model dates were earliest Devonian to latest Early Mississippian. These results compare well with those of previous work.

Glauconites dated in this study have not remained closed systems with respect to rubidium and strontium throughout geologic time, and are therefore not suitable for dating by the Rb-Sr method. Addition of rubidium to or loss of strontium from the glauconite crystal lattice may have resulted from allogenic recrytallization of the glauconite. Fluids which may have circulated through the limestone after glauconite genesis probably acted as a vehicle for rubidium addition and strontium loss.

INTRODUCTION

Geology of Västergötland

Miogeosynclinal sediments deposited in shallow epicontinental seas are preserved as a nearly complete lower Cambrian to lower Silurian sequence in Västergötland, south-central Sweden (Figure 1). The sequence is deposited on Archean gneiss eroded to a sub-Cambrian peneplain, and overlain by a dolerite caprock which was originally intruded as a sill after deposition of lower Silurian sediments. The entire sequence in Västergötland is virtually horizontal and has a maximum stratigraphic thickness of about 220 meters. The resistant dolerite caprock, together with high-angle normal faults which post-date sill intrusion, preserve the easily erodable Cambro-Silurian rocks (Figure 1).

The Cambrian strata are lithologically similar where the sequence is preserved (Figure 2). These rocks consist of a basal conglomeratic sandstone unit derived from the Scandinavian Baltic Shield, which is overlain by a kerogen-rich unit refered to as the alum shale. The alum shales are intercalated with bituminous limestones, locally refered to as stinkstone.

Ordovician and lower Silurian sediments consist of intertongueing units of marine limestone and shale. Limestone dominates the lithology southeast of Västergötland, while these rocks become shalier west and south.

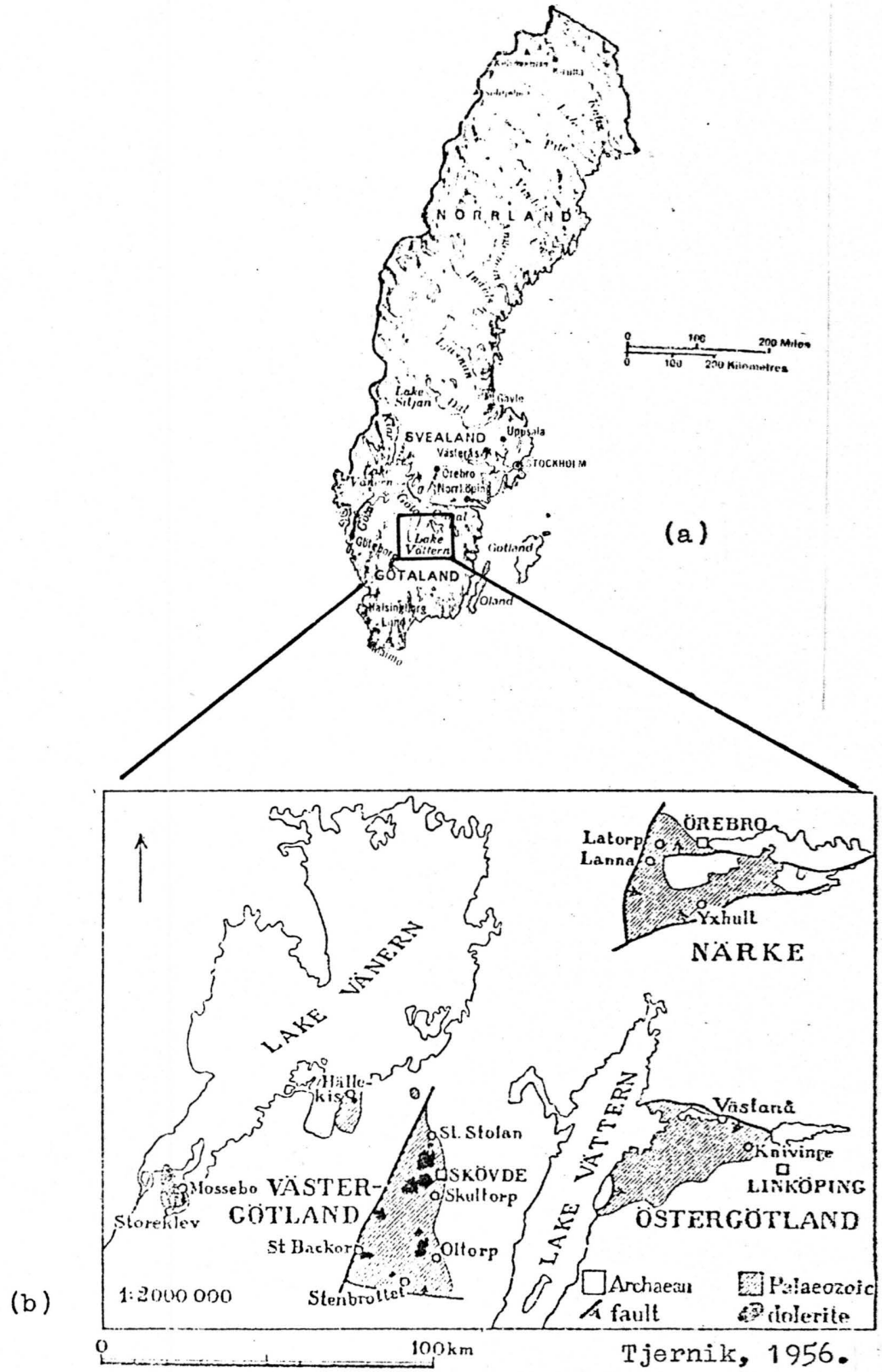

Figure 1. Sketch map of Sweden (a) with maps of larger scale showing Västergötland and Stenbröttet (b), the geology near Stenbröttet (c), and a cross section across map (c) showing the dolerite caprock and high angle normal faults (d).

(c)

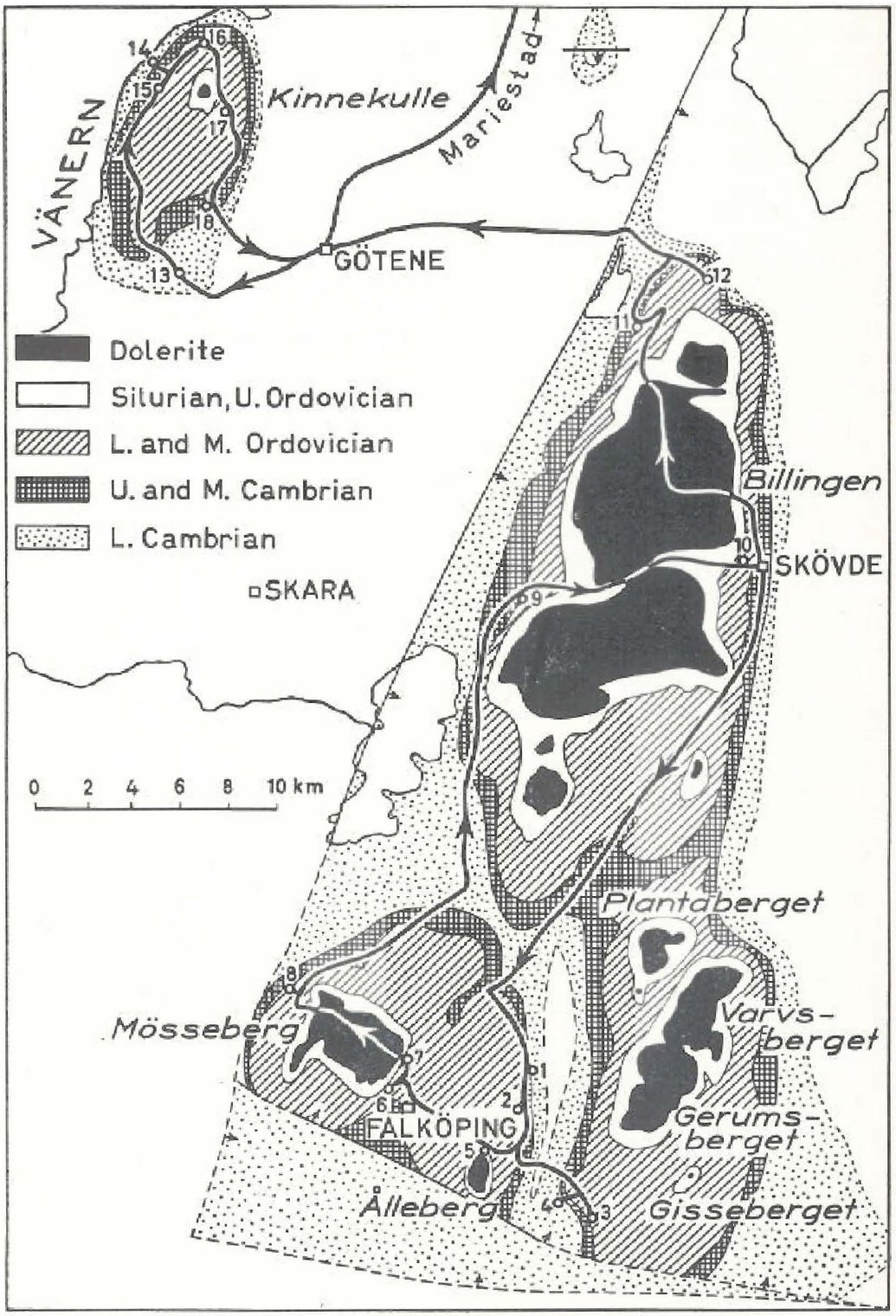

Map of Mt Kinnekulle and the Billingen-Falbygden district. After H. Munthe.

(d)

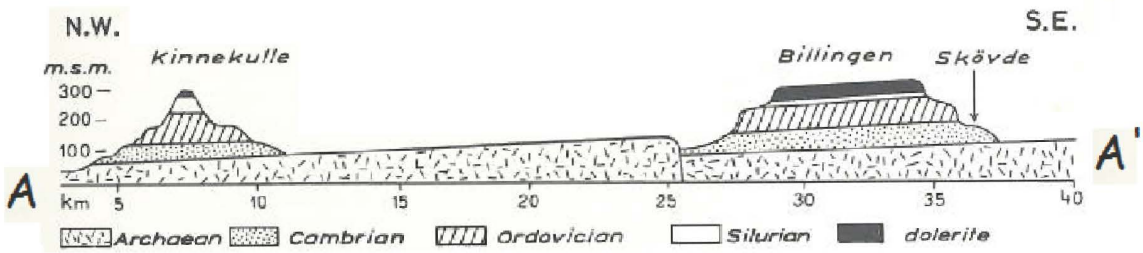

Thorslund, 1960.

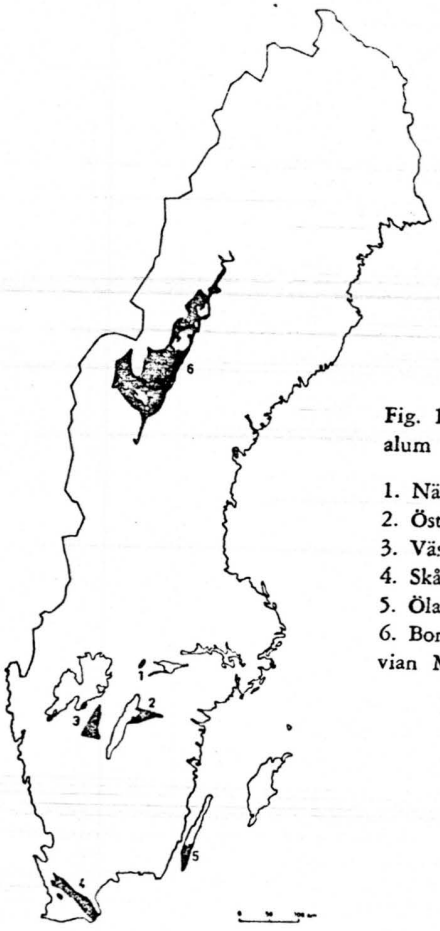

Fig. 1. The distribution of alum shales in Sweden

1. Närke
2. Östergötland
3. Västergötland
4. Skåne
5. Öland
6. Border of the Scandinavian Mountain Range.

Armando, 1973.

Figure 2. Sketch map of Sweden showing the actual distribution of alum shales, and indirectly the approximate distribution of Cambro-Silurian strata.

The Lower Ordovician

The lower Ordovician rocks in Västergötland consist of interbedded thin-bedded glauconitic limestone and glauconitic shale. Deposition occurred during intermittent west to east transgression (Thorslund, 1960). Biostratigraphic division of the lower Ordovician in southern Sweden is based on trilobite and graptolite facies-zones (Thorslund, 1960), and more recently by conodant zones (Lindström, 1971a; Bergström, 1971, 1973a, 1977) (Figure 3,4).

Sample Locality

Lowermost Ordovician glauconitic limestone samples 447, 448 and 449 were collected by Dr. Stig Bergström from a quarry wall near Stenbröttet in 1966. Stenbröttet is located approximately 10 kilometers southeast of Folkoping (Figure 1c, Stop 3). The stratigraphic succession of the lowermost Ordovician at the Stenbröttet locality, and the equivalent stratigraphic positions from which the samples were collected, is illustrated in Figure 5. Sample 447 was collected from the top 5 cm of the basal Arenigian Planilimbata limestone; sample 448 from a position 10 cm above the base of the basal Arenigian Phyllograptus densus zone; sample 449 from a position 0-10 cm above the top of the top of the Cambrian in the Lower Tremadocian Ceratopyge limestone.

CAMBRIAN

Upper Cambrian Olenid Series	*Acerocare*	
	Peltura scarabaeoides	
	Peltura minor	
	Protopeltura praecursor	
	Leptoplastus and *Eurycare*	
	Parabolina spinulosa and *Orusia*	
	Olenus and *Agnostus obesus*	
	Agnostus pisiformis	
Middle Cambrian *Paradoxides* Series	*Forch-hammeri* stage	*Lejopyge laevigata*
		Solenopleura brachymetopa (Andrarum Limestone)
		Ptychagn. lundgreni and *Goniagn. nathorsti*
	Paradox-issimus stage	*Ptychagn. punctuosus*
		Hypagn. parvifrons
		Tomagn. fissus and *Ptychagn. atavus*
		Ptychagn. gibbus
	Oelandicus stage	*Paradoxides pinus*
		Paradoxides insularis
Lower Cambrian Series	*Strenuella linnarssoni*	
	Holmia kjerulfi	
	Volborthella and *Platysolenites*	
	Discinella holsti	

Thorslund, 1960.

Figure 3.

Cambrian, Ordovician and Silurian biostratigraphic subdivsion of the geologic time scale in Sweden, showing trilobite and graptolite facies-zones.

SILURIAN

England	Graptolite zones	Scania	Västergötland (Kinnekulle)	Dalecarlia	Jämtland	Gotland
Ludlow	(Graptolitic facies unknown in Sweden)	Öved-Ramsåsa (100 – 300 m.)		? Orsa sandstone ?		Sundre 10m, Hamra 40, Burgsvik 50, Eke 15, Hemse 100, Klinteberg 100, Mulde 25, Halla 15, Slite 100, Tofta 10, Högklint 35
	Monogr. scanicus	*Colonus* shale (c. 600 m.)				
	" *nilssoni*					
Wenlock	*Cyrtogr. lundgreni* and *Monogr. testis*	*Cyrtograptus* shale (c. 350 m.)		*Bumastus limesi*	Ekeberg greywacke	
	Cyrtogr. rigidus			Stygglors "	?	Upper Visby 15
	Monogr. riccartonensis			*Retiolites* shale	Bångsåsen shales	Lower Visby
	Cyrtogr. murchisoni					Grey mudstone
Llandovery Upper	" *tapworthi*		*Retiolites* shale (26 m.)			Red " "
	Monogr. spiralis					
	" *discus*	*Rastrites* shale (c. 120 m.)	*Rastrites* shale (29.4 m.)	*Rastrites* shale (c. 50 m.)	Berge limestone	Mudstone and limestone
	" *turriculatus*					
	" *sedgwicki*					
Middle	*Cephalogr. cometa*					
	Petalolithus folium				Ede quartzite	Hiatus
Lower	*Monogr. gregarius*			Poorly fossiliferous grey and red marly shales ?		
	" *revolutus*					
	Rhaphidogr. extenuatus				? Upper Kyrkås	
	Akidogr. acuminatus					
	Glyptogr. persculptus					

ORDOVICIAN

	England	Shelly facies	Graptolitic facies	
Upper Ordovician	Ashgill	*Dalmanitina* beds, *Staurocephalus* beds, *Trinucleus* limestone and shales, *Standrom* limestone (Boda)		Unknown
			Upper	*Dicellogr. complanatus*, *Climacogr. styloideus*
	Caradoc	*Macrourus* limestone (Kullsberg), *Ludibundus* —"—, *Crassicauda* —"—, *Schroeteri* —"—, *Platyurus* —"—	Middle	*Dicranogr. clingani*, *Nemagr. gracilis*
Middle Ordovician	Llandeilo		Lower	*Glyptogr. teretiusculus*
	Llanvirn	*Vaginatum*: *Gigas* —"—, *Obtusicauda* —"—, *Raniceps* —"—, *Expansus* —"—	Upper	*Didymogr. murchisoni*, *Didymogr. bifidus*
Lower Ordovician	Arenig	*Lepidurus* —"—, *"Limbata"* —"—	Lower	
		Billingen: *Estonica* —"—, *Dalecarlicus* —"—		*Isograptus gibberulus*, *Phyllogr. angustifolius elongatus*, *Phyllograptus densus*, *Tetragr. phyllograptoides*
		Hunneberg: *Planilimbata* —"—, *Armata* —"—	?	Unknown
		Ceratopyge limestone, *Ceratopyge* shale	? *Clonograptus* shale	? *Clonogr. hares*
	Tremadoc	*Obolus* beds	*Dictyonema* shale	*Dictyonema norvegicum*, *Dictyonema desmograptoides*

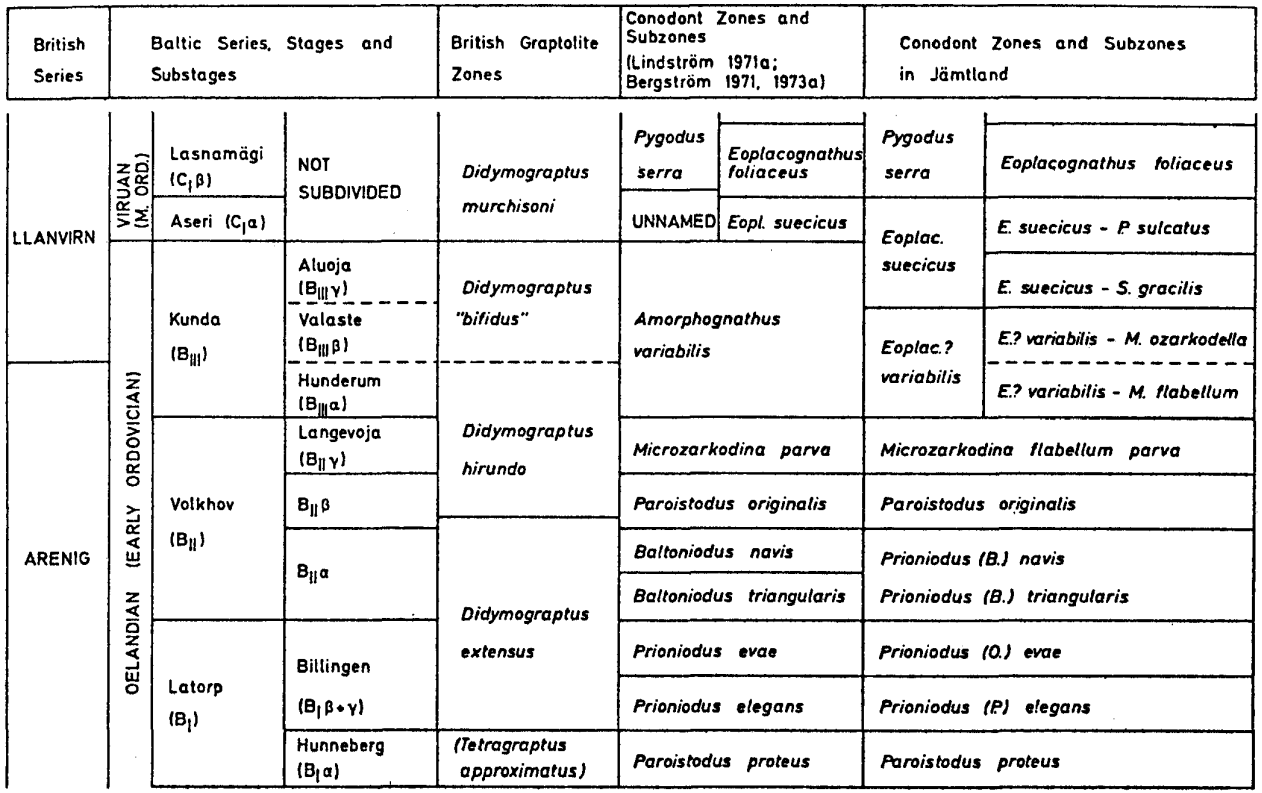

Fig. 1. Correlation between main stratigraphic units discussed in this report. Based mainly on Lindström (1971a) and Bergström (1971, 1973a, 1977a).

Löfgren, 1978.

Figure 4. Subdivision of the Early Ordovician by conodant zones and subzones.

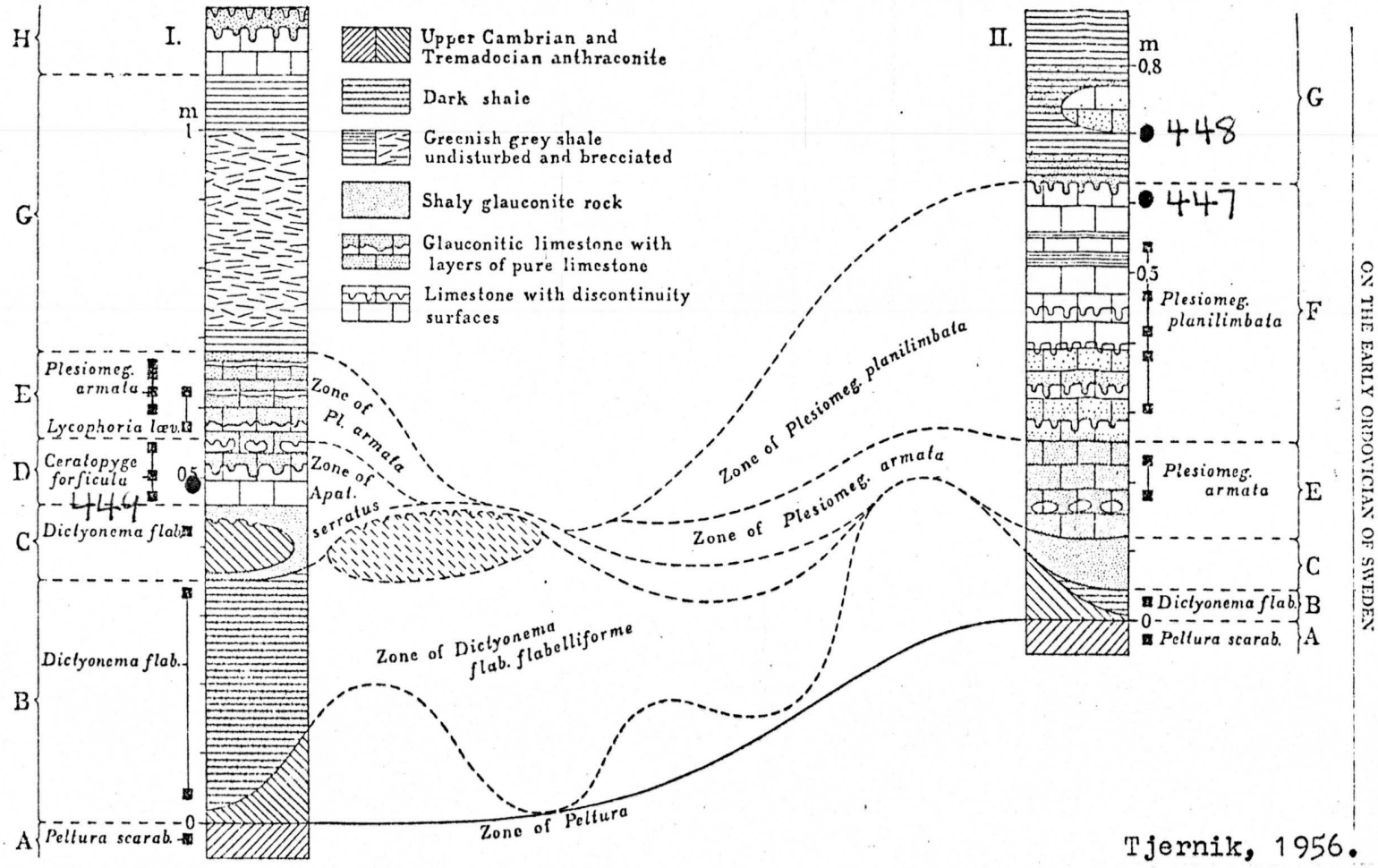

Sections I and II through the lowermost Ordovician beds at Stenbrottet, Västergötland.

Figure 5. Diagramatic sketch of the stratigraphic detail from the quarry near Stenbröttet, with approximate stratigraphic positions from which the glauconitic limestone samples were collected.

MINERALOGY OF GLAUCONITE

Chemical Composition and Internal Structure

Glauconite is a hydrous aluminum silicate mineral and has the following general chemical composition:

$$K_2(Mg,Fe)_2Al_6(Si_4O_{10})_3(OH)_{12}$$

(Hurlbut, 1971). Rubidium cations, which are monovalent and have an ionic radius of 1.48 Å, may substitute for potassium cations, which are also monovalent and have an ionic radius of 1.33 Å. This substitution of rubidium cations for potassium cations takes place at the site in the interlayered smectite(montmorillonite)-illite clay mineral sheet structure of potassium cation adsorbtion (Grim, 1968). Strontium cations may also occupy this position in the crystal lattice (Figure 6). Adsorbtion of alkali and alkaline earth cations onto the basal planes within the smectite and illite lattice-layer types in the mineral glauconite occurs because aluminum cations (Al^{+3}) are replacable by iron and magnesium cations (Fe^{+3}, Fe^{+2}, Mg^{+2}). The octahedral and tetrahedral sites in the crystal lattice become negatively charged when this replacment occurs, and adsorbtion of alkali and alkaline earth cations takes place at the sites of negative charge (Kazakov and Palevaya, 1958).

Genesis of Glauconite

Velde and Odin (1975) distinguished glauconite-

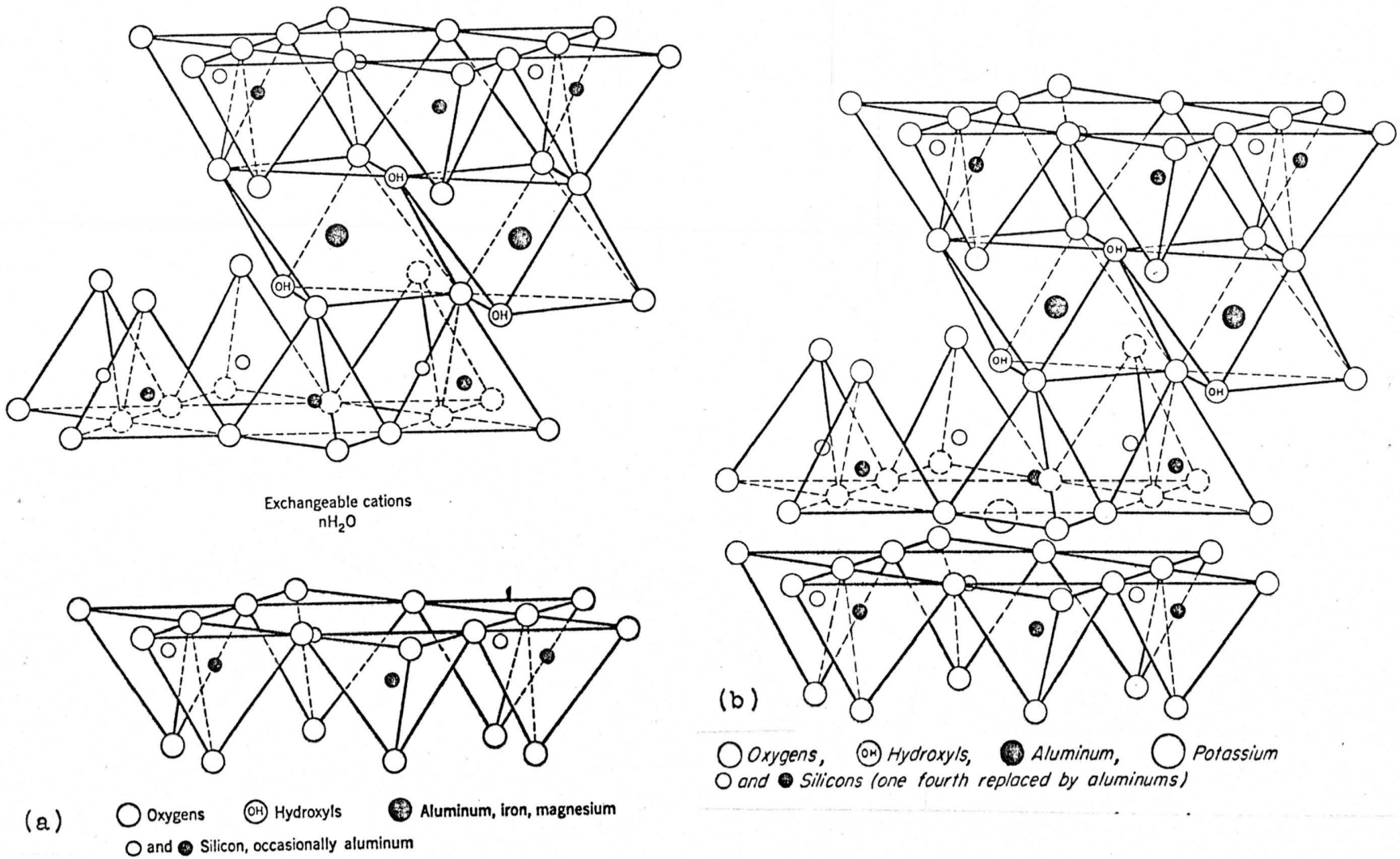

Figure 6. Diagramtic sketch of clay mineral layer types, showing the expandable smectite (monmorillonite) (a) and non-expandable illite (b) crystal lattice sheets. Grim, 1968.

smectite from illite-smectite mixed-layered clay minerals by the differences in potassium and iron content in the two mineral types. Their findings indicate that when detrital or chemical crystal nuclei contain mixed-layered mica-smectites (detrital micas or slightly crystallized colloidal alumina or silica) temperature increases produce an iron-rich mica in the case of glauconite, and an aluminous mica in the case of illite.

Logvinenko and others (1975) advocate a multiple-stage genesis of glauconite in which the initial material is a poorly crystallized single-layer hydrous mica of polytype 1Md with a significant admixture of a mixed-layered phase of hydrous mica or montmorillonite. This initial material contains more than 30% swollen layers. With time, this material transforms into a more crystallized single-layered dioctahedral hydrous mica of polytype 1M with some remaining admixture of the mixed layered phase of hydrous mica and monmorillonite, with only 10-20% swollen layers.

Sorption of Cations

Associated with the crystochemical decrease in the number of swollen layers with time is a continued increase in the sorption of alkali (K, Rb) and alkaline earth (Sr) elements (Hurley et al., 1960). Hurley and

others noted both the associated occurrence of increased alkali-fixation (Rb, K) with a decrease in the percentage of expandable layers in lower Paleozoic glauconites, and that common strontium is adsorbed to the basal surfaces of the expandable (smectite) layers and is easily removed by exchange.

Hurley and others (1960) observed that the potassium content of glauconites is inversely proportional to the percentage of expandable layers. When the percent of expandable layers decreases from an initial 30% to 10-20% with time, the potassium content increases. This observation is significant in that since rubidium may substitute for potassium in glauconite, it now becomes reasonable to assume that the rubidium content also increases with time.

ANALYTICAL METHODS

Introduction

Age determinations by the Rb-Sr method of dating require measurement of the concentration of rubidium and strontium, and of the $^{87}Sr/^{86}Sr$ ratio of the mineral. The concentrations can be determined by X-ray fluorescence, while the $^{87}Sr/^{86}Sr$ ratio is determined by isotope analysis of the strontium by mass spectrometry.

The age of a rubidium-bearing mineral such as

glauconite is calculated by use of an equation derived from the law of radioactivity :

$$t = \frac{1}{\lambda} \ln \left[\frac{^{87}Sr/^{86}Sr - (^{87}Sr/^{86}Sr)_o}{^{87}Rb/^{86}Sr} + 1 \right] \qquad (1)$$

where t is a date in the geologic past, λ is the decay constant for ^{87}Rb equal to $1.42 \times 10^{-11} y^{-1}$ (Neumann and Huster, 1974), $^{87}Sr/^{86}Sr$ is the ratio of strontium isotopes at the time of the analysis, $(^{87}Sr/^{86}Sr)_o$ is the initial ratio of $^{87}Sr/^{86}Sr$ at the last time the glauconite crystal lattice became closed to rubidium and strontium, and $^{87}Rb/^{86}Sr$ is the ratio of ^{87}Rb to ^{86}Sr in the sample at the time of the analysis.

The calculated date, t, is the 'age' of the mineral only if: (1) the glauconite has remained a closed system with respect to rubidium and strontium; (2) the assumed value of the initial $^{87}Sr/^{86}Sr$ ratio is appropriate, and (3) the analytical results are accurate and representative of the material to be dated (Faure, 1977). Since glauconite is initially formed authigenically in a marine environment (Grim, 1968; Logvinenko et al., 1975; Velde and Odin, 1975), the initial $^{87}Sr/^{86}Sr$ ratio is assumed to be equal to the $^{87}Sr/^{86}Sr$ of the marine water in which the mineral formed. The initial $^{87}Sr/^{86}Sr$ ratio for glauconite samples analyzed in this study is assumed to be identical to that of marine carbonate rocks

of lower Ordovician age. An average $^{87}Sr/^{86}Sr$ ratio of 0.708 has been obtained from analyses on a few carbonate rocks of lower Ordovician age (Faure et al., 1978). This value was substituted into equation (1) during the calculation of t.

The value of the $^{87}Rb/^{86}Sr$ ratio at the time of analysis was calculated by use of the following equation:

$$\frac{^{87}Rb}{^{86}Sr} = \left(\frac{Rb}{Sr}\right) \frac{Ab^{87}Rb \times WSr}{Ab^{86}Sr \times WRb} \qquad (2)$$

where (Rb/Sr) is the ratio of the total concentration of rubidium and strontium in parts per million in the sample as determined from X-ray fluorescence; $Ab^{87}Rb$ is the isotopic abundance of naturally occurring ^{87}Rb equal to 27.8346 atom percent; WSr is the atomic weight of strontium in the sample as determined from the isotope analysis; $Ab^{86}Sr$ is the isotopic abundance of ^{86}Sr in the sample as determined from isotope analysis; and WRb is the atomic weight of Rb equal to 85.46776 amu (Catanzaro et al., 1969). The date in the geologic past when a given glauconite grain became a closed system to rubidium and strontium may be calculated after the rubidium and strontium concentrations and the $^{87}Sr/^{86}Sr$ ratio are measured.

X-ray Fluorescence Calibration

Strontium and rubidium concentrations in the

glauconite samples could be determined only after the spectrometer was calibrated. Calibrations were made with U. S. Geological Survey rock standards: G-2, GSP-1, BCR-1, AVG-1, and W-1 (Flanagan, 1973), and intralaboratory monitor 48R3.* A Diano Corporation XRD-6 air path spectrometer using MoK-alpha radiation, a LiF diffracting crystal cut parallel to the (220) crystallographic plane, and a scintillation detector, was operated at an accelerating voltage of 65 KVP and a current of 45 ma, with a Soller slit setting of 0.10 inches. The instrument was allowed to stabilize at these operational settings prior to actual analyses. Care was taken to insure that internal allignment of the LiF diffracting crystal was correctly adjusted to 35.85 degrees two theta (Table I, Figure 7).

Intralaboratory monitor 48R3 was analyzed before and after five consecutive sets of three U.S.G.S. rock standards in order to monitor drift in the instrument settings during the calibration. Peak and baseline intensities, as well as the MoK-alpha Compton scattered intensity ($MoK_{\alpha}C$), were measured for each rock standard and monitor 48R3 for specified periods of time and degree-2θ values as shown in Table 2. Matrix corrections were made by dividing the net Sr and net Rb

* Coldwell Complex syenite, north shore of Lake Superior

Table I. Internal allignment of the LiF diffracting crystal was checked by recording intensity counts at goniometer settings slighty above and below 35.85 degrees 2θ.

Degrees 2θ	10 second counts			Average
35.70	638	647	644	643
35.75	639	708	708	685
35.80	750	747	725	741
35.85	742	751	757	750
35.90	737	752	753	747
35.95	720	701	714	712

Table 2. Peak and baseline intensities, and MoK-alpha Compton scattered intensity, of fluoresced X-rays from each rock standard and monitor 48R3 measured during calibration.

X-ray Intensity	Degrees 2θ	Count Time (sec)
MoK$_\alpha$C	30.00	100
Baseline 1	35.20	100
SrK$_\alpha$	35.85	200
Baseline 2	36.50	100
RbK$_\alpha$	37.99	200
Baseline 3	38.58	100

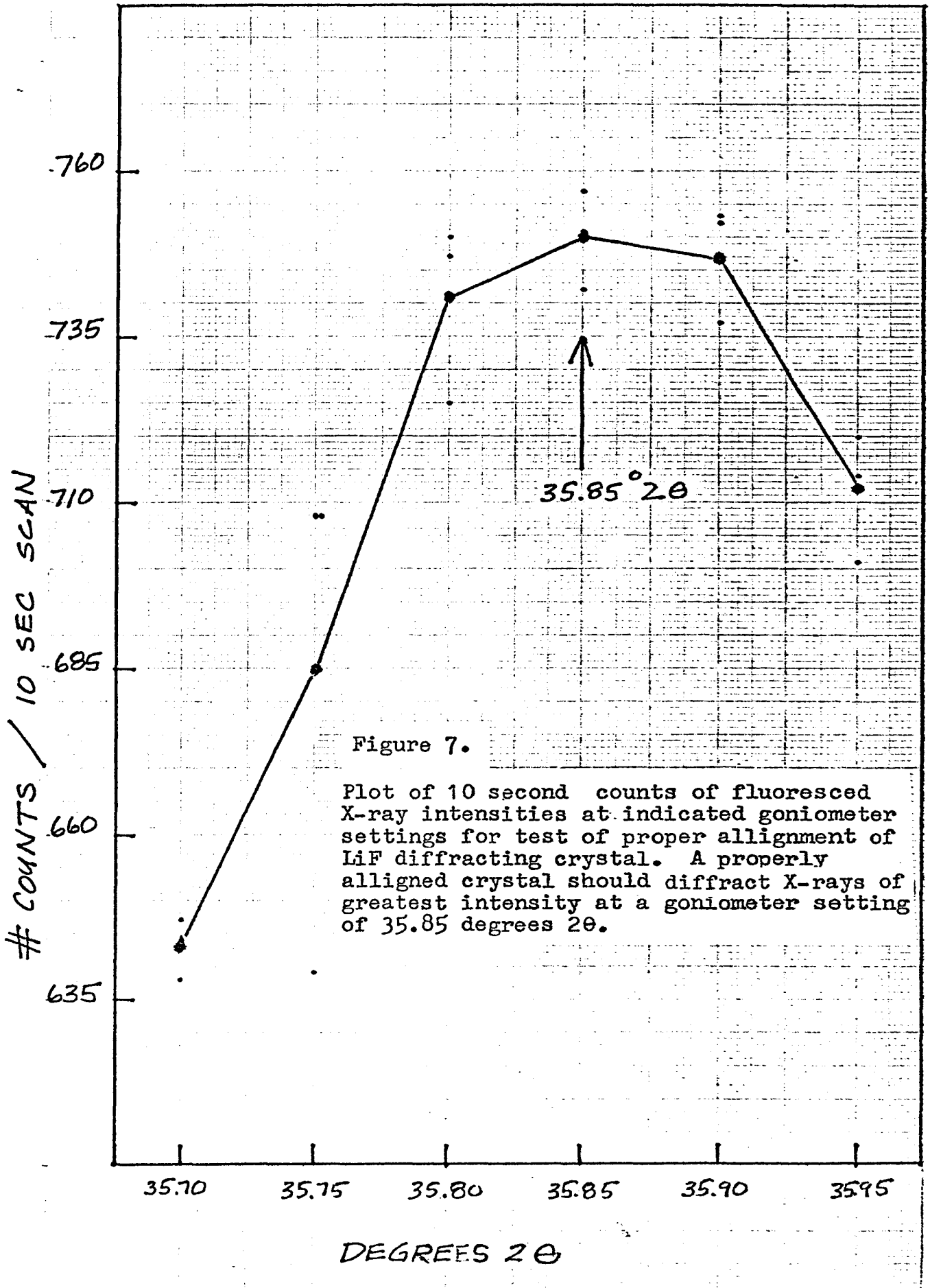

Figure 7.

Plot of 10 second counts of fluoresced X-ray intensities at indicated goniometer settings for test of proper allignment of LiF diffracting crystal. A properly alligned crystal should diffract X-rays of greatest intensity at a goniometer setting of 35.85 degrees 2θ.

intensities by the intensities of $MoK_{\alpha}C$ (Reynolds, 1963). Matrix-corrected values of net Sr and net Rb were multiplied by an instrument drift correction factor, f. The drift was assumed to have been linear between matrix-corrected values of net Sr and net Rb peak intensities of monitor 48R3, and drift correction factors were found by interpolation of net $Sr/MoK_{\alpha}C$ or net$Rb/MoK_{\alpha}C$ values for anytime t during the analysis. The arbitrarily chosen values of net $Sr/MoK_{\alpha}C$ and net $Rb/MoK_{\alpha}C$ to which the drift correction factors were interpolated were 0.3150 and 0.1325, respectively (Figure 8).

Calibration equations were determined by least squares regression analysis; the regression lines were forced through the origin (Figure 9, 10). This analysis yielded the following calibration equations:

$$\text{Sr ppm} = 610.468\left(\frac{\text{net Sr}}{MoK_{\alpha}C}\right)^{c} + 0.039 \qquad (3)$$

$$\text{Rb ppm} = 816.345\left(\frac{\text{net Rb}}{MoK_{\alpha}C}\right)^{c} + 0.038 \qquad (4)$$

where $(\text{net } Sr/MoK_{\alpha}C)^{c}$ and $(\text{net } Rb/MoK_{\alpha}C)^{c}$ are matrix-corrected values of net Sr and net Rb peak intensities corrected for instrument drift. Calibration equations (3) and (4) were used to calculate Sr and Rb concentrations in glauconite samples 447, 448 and 449.

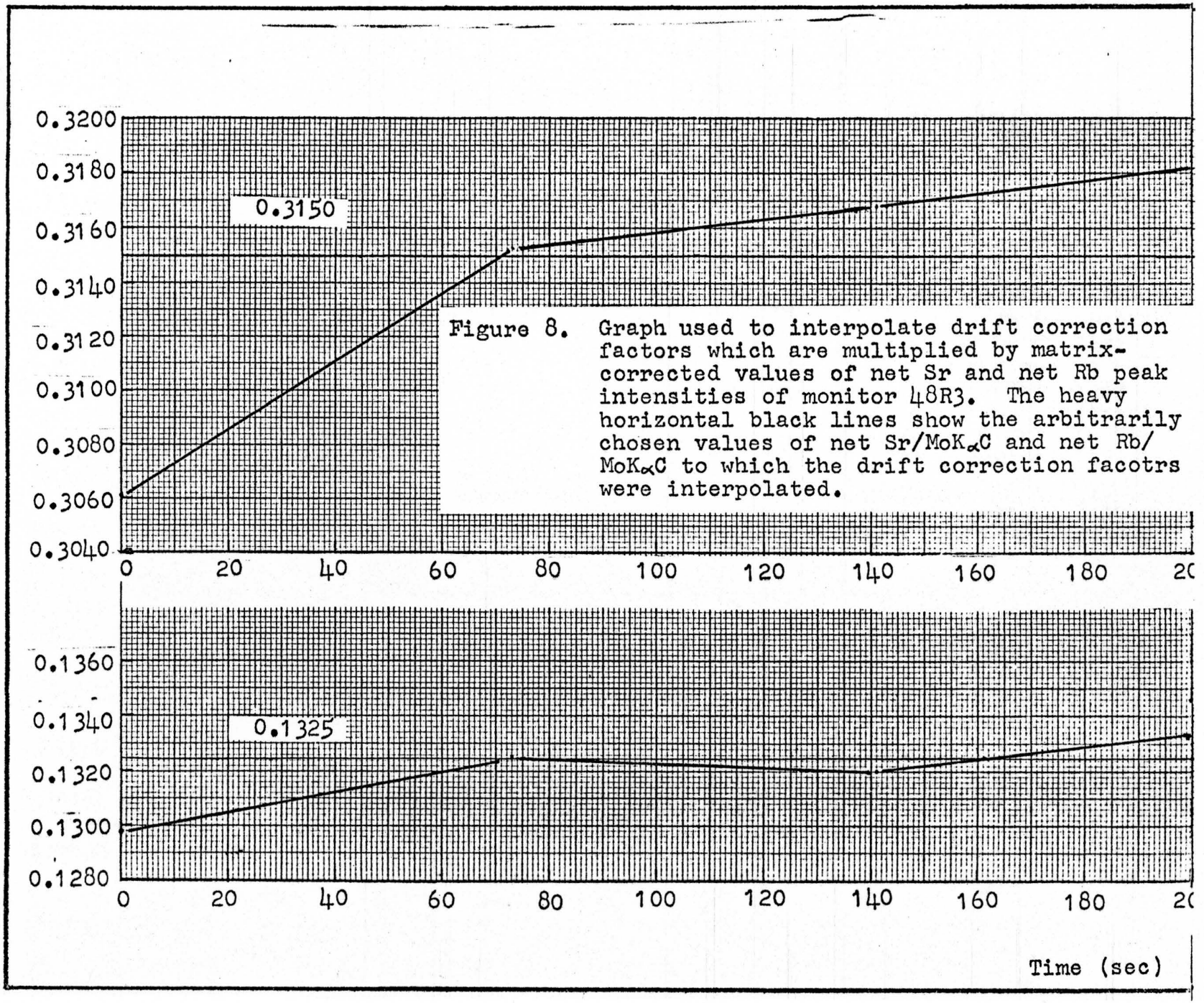

Figure 8. Graph used to interpolate drift correction factors which are multiplied by matrix-corrected values of net Sr and net Rb peak intensities of monitor 48R3. The heavy horizontal black lines show the arbitrarily chosen values of net Sr/MoK$_\alpha$C and net Rb/MoK$_\alpha$C to which the drift correction facotrs were interpolated.

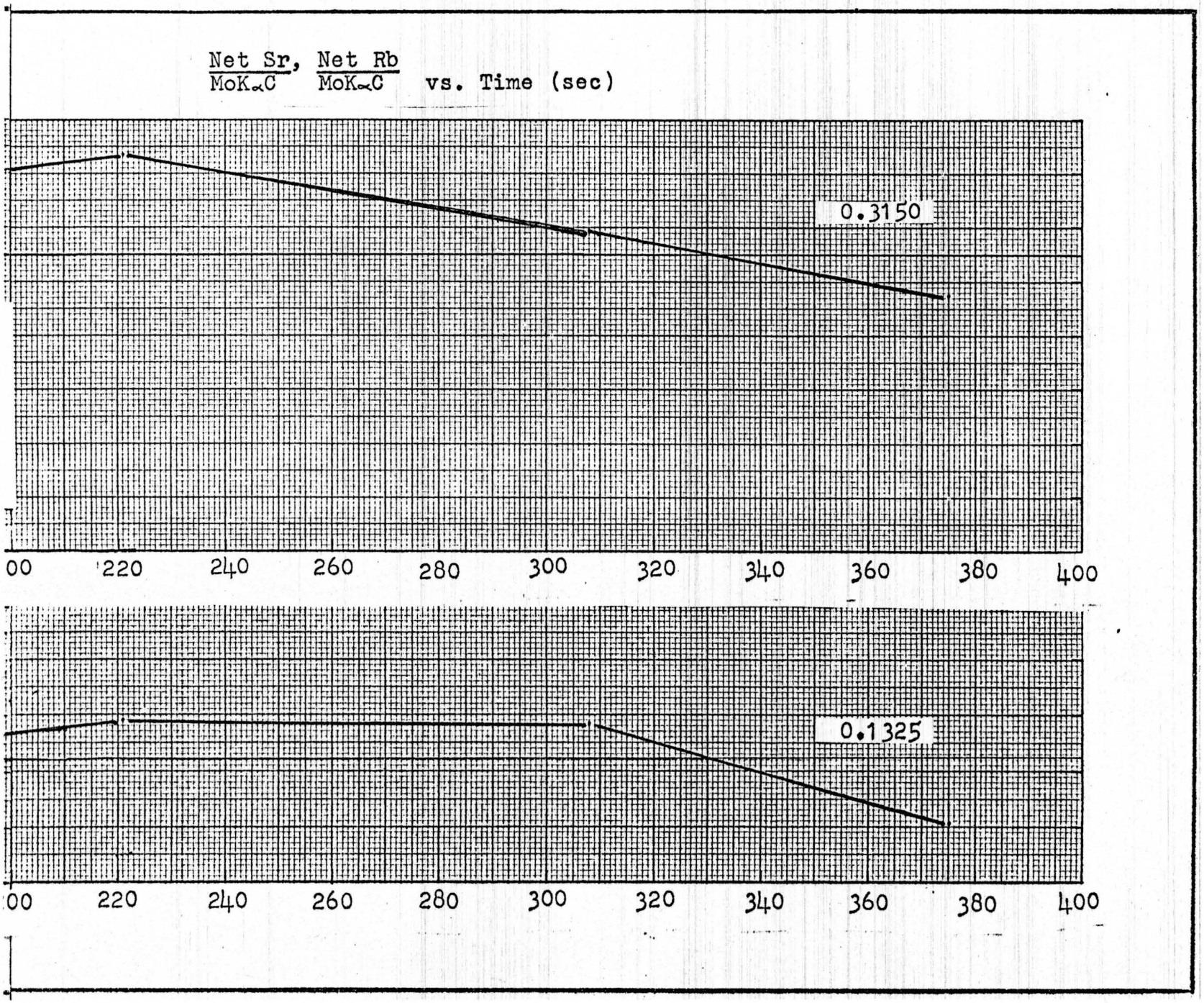
Net Sr / MoKαC Net Rb / MoKαC vs. Time (sec)
0.3150
00
220
240
260
280
300
320
340
360
380
400
0.1325
00
220
240
260
280
300
320
340
360
380
400

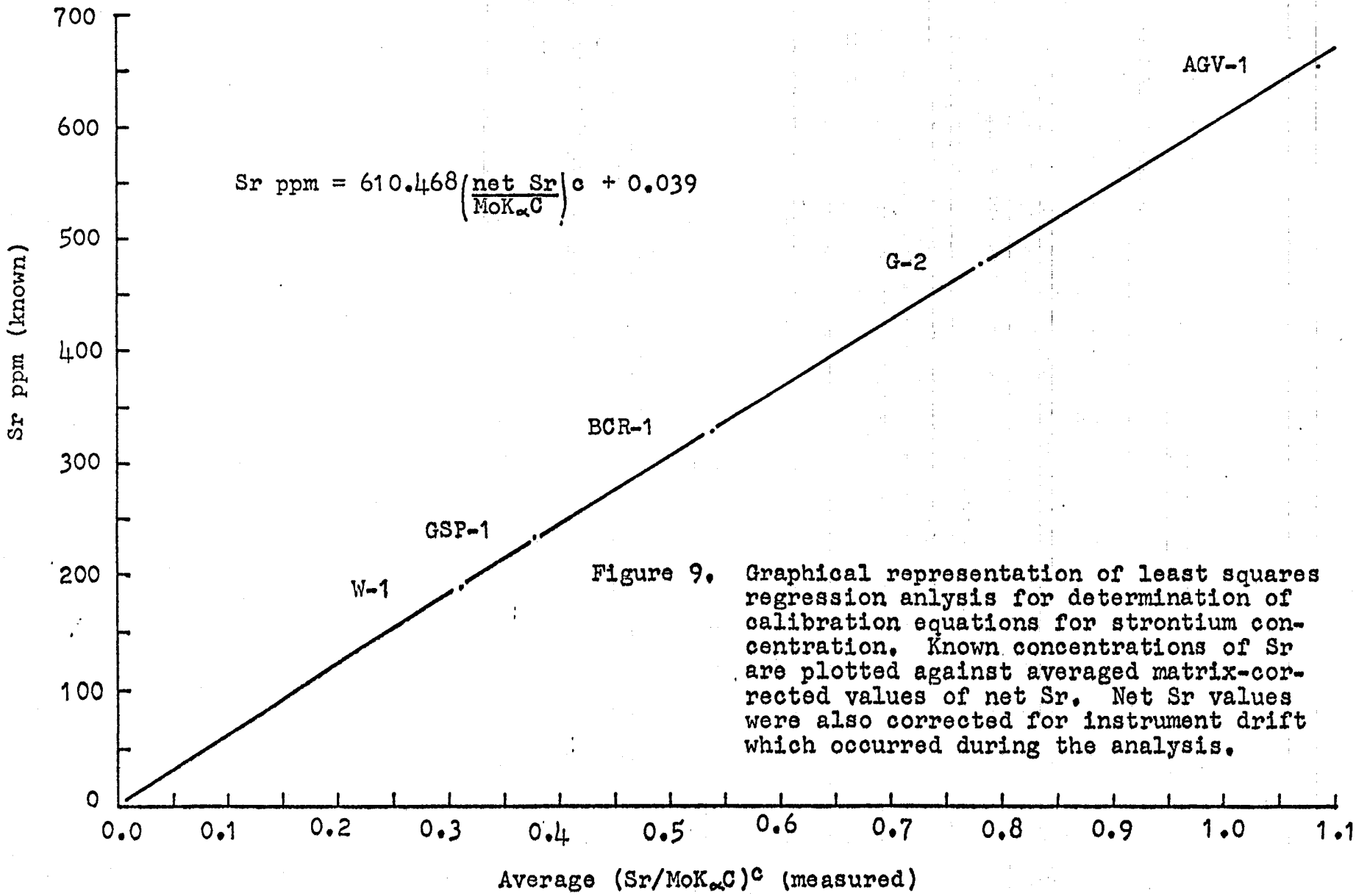

Figure 9. Graphical representation of least squares regression anlysis for determination of calibration equations for strontium concentration. Known concentrations of Sr are plotted against averaged matrix-corrected values of net Sr. Net Sr values were also corrected for instrument drift which occurred during the analysis.

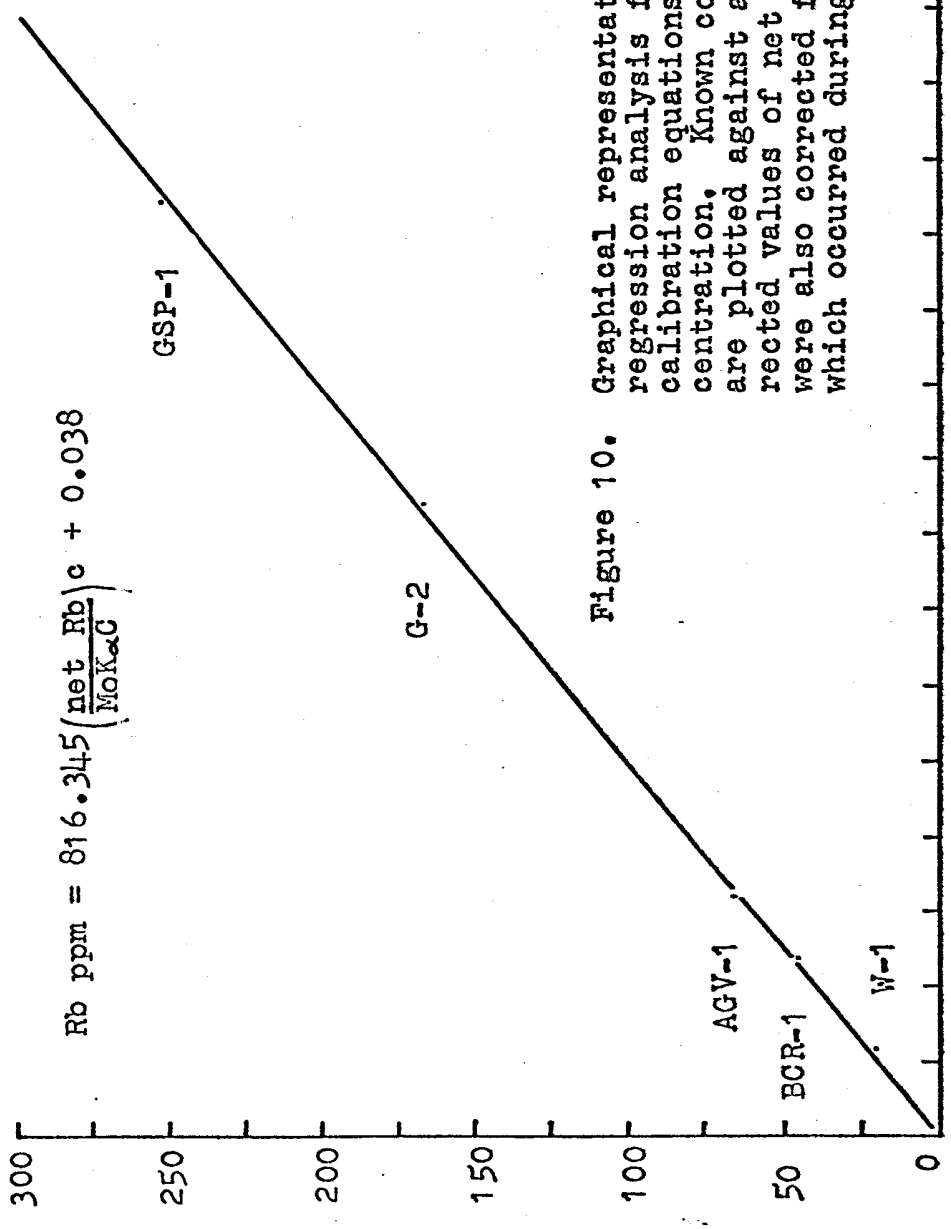

Figure 10. Graphical representation of least squares regression analysis for determination of calibration equations for rubidium concentration. Known concentrations of Rb are plotted against averaged matrix-corrected values of net Rb. Net Rb values were also corrected for instrument drift which occurred during the analysis.

X-ray Fluorescence of Glauconite

Glauconite was separated from the limestone host rock by grinding in an iron mortar and pestle to a particle size of -60 to +120 mesh per inch. Glauconite from this size fraction was separated magnetically and subsequently powdered in a clean agate mortar until the powder passed a -200 mesh sieve. Approximately 3 grams of powdered glauconite, backed by 6 to 7 grams of boric acid crystals, was compressed into a pellet in a hydraulic press. These pellets are suitable for study by X-ray fluorescence. Samples 447, 448 and 449 were analyzed in the same manner as were the U.S.G.S. rock standards during the calibration. Intralaboratory monitor 48R3 was analyzed before and after two sets of all three glauconite samples twice, for a total of four sets of data per sample. Instrument drift was again assumed to have been linear between values of matrix-corrected net Sr and net Rb of the monitor. Drift correction factors used for correcting glauconite sample values of matrix-corrected net Sr and net Rb were interpolated from the graph shown in Figure 11. Rubidium and strontium concentrations are listed with $^{87}Rb/^{86}Sr$ and $^{87}Sr/^{86}Sr$ ratio values in Table 3.

Strontium Isotope Analysis

A Nuclide Corporation Model 6-60-S mass spectrometer

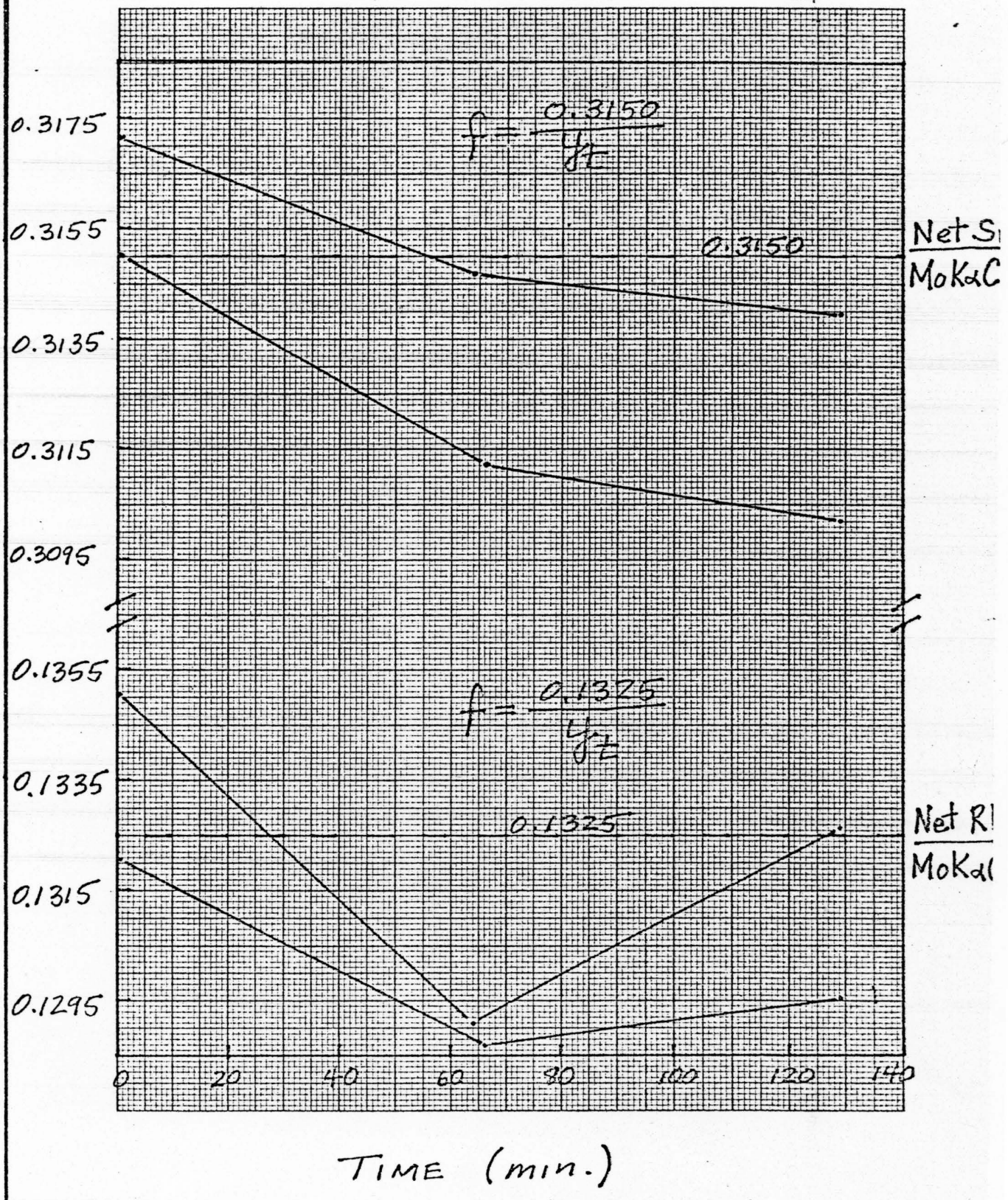

Figure 11. Graph from which drift correction factors used for correcting glauconite sample values of matrix-corrected net Sr and net Rb were obtained. The arbitrarily chosen values of net Sr (0.3150) and net Rb (0.1325) to which the drift correction factors were interpolated are necessarily the same as those used in the calibration.

Table 3. Data generated from X-ray fluorescence and Sr isotope analyses on glauconites 447, 448 and 449 for Rb-Sr model date calculation.

Sample	Sr ppm	Rb ppm	WSr	$Ab^{87}Sr$	$^{87}Sr/^{86}Sr$	$^{87}Rb/^{86}Sr$	t years
447	18.389	281.695	87.60438	0.09584	0.9202	45.54535	327×10^6
448	26.168	284.385	87.60407	0.09670	0.8881	32.02412	395×10^6
449	21.273	279.122	87.60432	0.09188	0.9188	39.31450	376×10^6

was used to measure $^{87}Sr/^{86}Sr$ ratios. A pure strontium salt was obtained by dissolving powdered glauconite in acid, isolating the Sr in solution with cation exchange chromatography, and evaporating the resultant solution onto a tantalum filament. This filament was then used as a solid source for Sr isotopes in the mass spectrometer.

The mass spectrum of strontium was traced on a linear strip chart recorder at a constant scan rate. Figure 12 shows an example of a representative mass spectrum of strontium obtained from glauconite 447. The peak height above the baseline is proportional to the abundance of the strontium isotope represented by the peak.

Rb-Sr Model Date Calculation

Calculation of Rb-Sr model dates for glauconite samples used in this study is facilitated by substituting data from Table 3 into equation (1). Sample 447 illustrates the calculation:

$$t = \frac{1}{\lambda} \ln \left[\frac{^{87}Sr/^{86}Sr - (^{87}Sr/^{86}Sr)_o}{^{87}Rb/^{86}Sr} + 1 \right] \qquad (1)$$

$$t_{447} = \frac{1}{1.42 \times 10^{-11} y^{-1}} \ln \left[\frac{0.9202 - 0.708}{45.54535} + 1 \right]$$

$$t_{447} = 3.27 \times 10^{8} \text{ years.}$$

Values of t for glauconite samples 448 and 449 may be

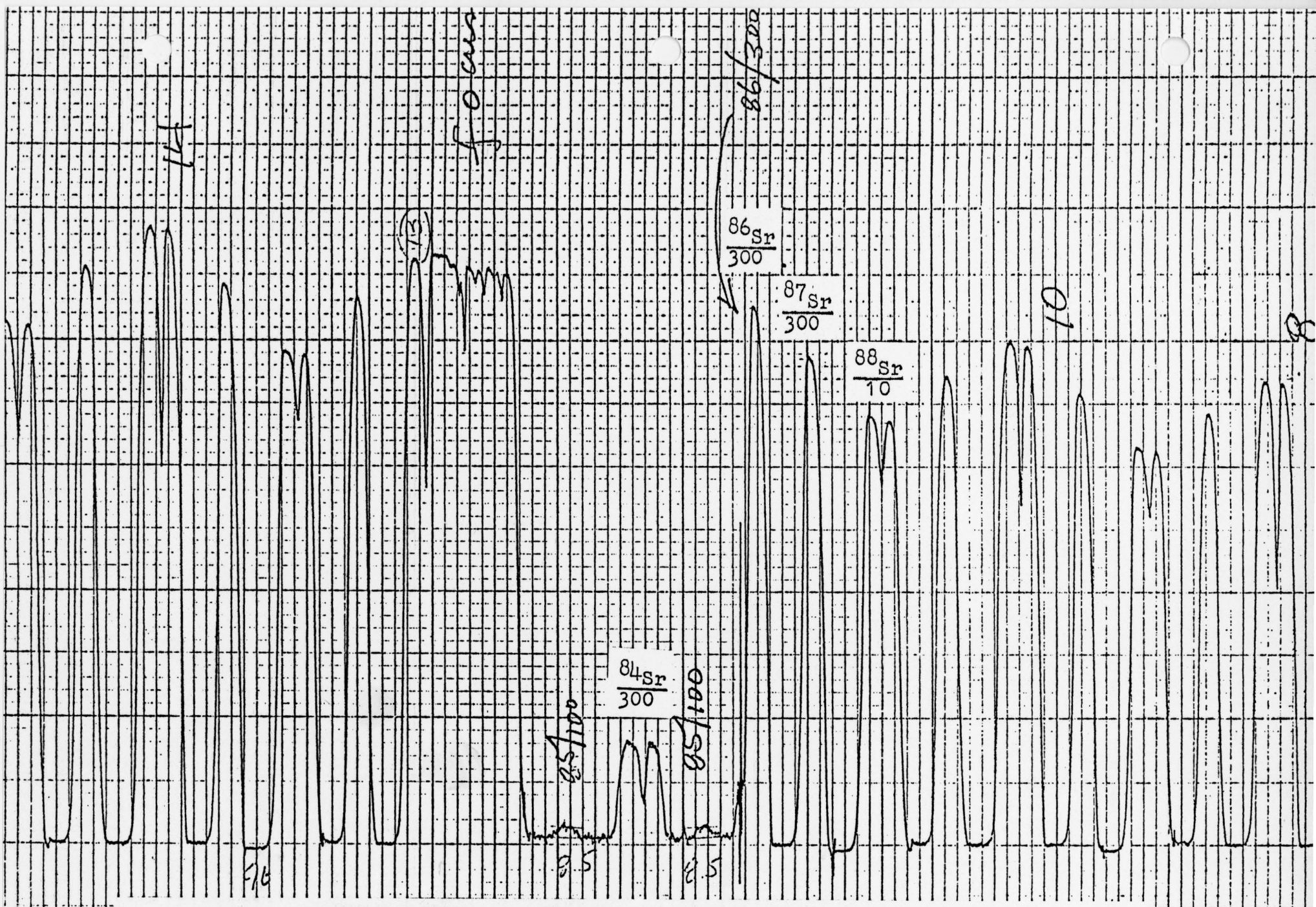

Figure 12. A representative mass spectrum of strontium from glauconite 447. The peak height above the baseline is proportional to the abundance of the strontium isotope represented by the peak.

found in Table 3.

RESULTS AND INTERPRETATIONS

Comparison with Previous Work

Rb-Sr age determinations made on glauconites from this study compare favorably with previous age determinations made on glauconites from the Stenbröttet locality (Figure 13). The average measured Rb concentrations from glauconites in this study are 9% lower than those of the earlier work. Conversely, the average measured Sr concentrations are 24% higher. Possible explanations for these discrepancies include: (1) the analytical methods used in this study differed markedly from those used in the earlier studies; (2) the samples were not collected from exactly the same positions in the quarry; or (3) the samples, as analyzed, differed in purity.

Rb-Sr Isochron Diagram

Model dates calculated in this study and an Early Ordovician reference isochron are plotted together on the Rb-Sr isochron diagram in Figure 14. The assumed Early Ordovician age of 485 million years was based on the work of Holmes(1959), Kulp(1961), Harland(1964), and Armstrong and McDowall(1974). Glauconites which formed 485 million years ago that have remained closed systems with respect to rubidium and strontium would plot

Figure 13. Table showing datafrom earlier Rb- Sr age determinations made on glauconites from the Stenbröttet locality.

Source	Sample	Rb ppm	Sr ppm	Rb/Sr	SrIR date
Herzog et al. 1958	G-11	307	16.7	18.4	375±29 my*
Hurley et al. 1960	G-3212	307	16.7	18.4	375±20 my**
This study 1978	447	281.695	18.389	15.3	327 my***
	448	284.385	26.168	10.9	395 my
	449	279.122	21.273	13.1	376 my
Average this study		281.730	21.943	12.8	366 my

* $\lambda = 1.47 \times 10^{-11} y^{-1}$
** $\lambda = 1.39 \times 10^{-11} y^{-1}$
*** $\lambda = 1.42 \times 10^{-11} y^{-1}$

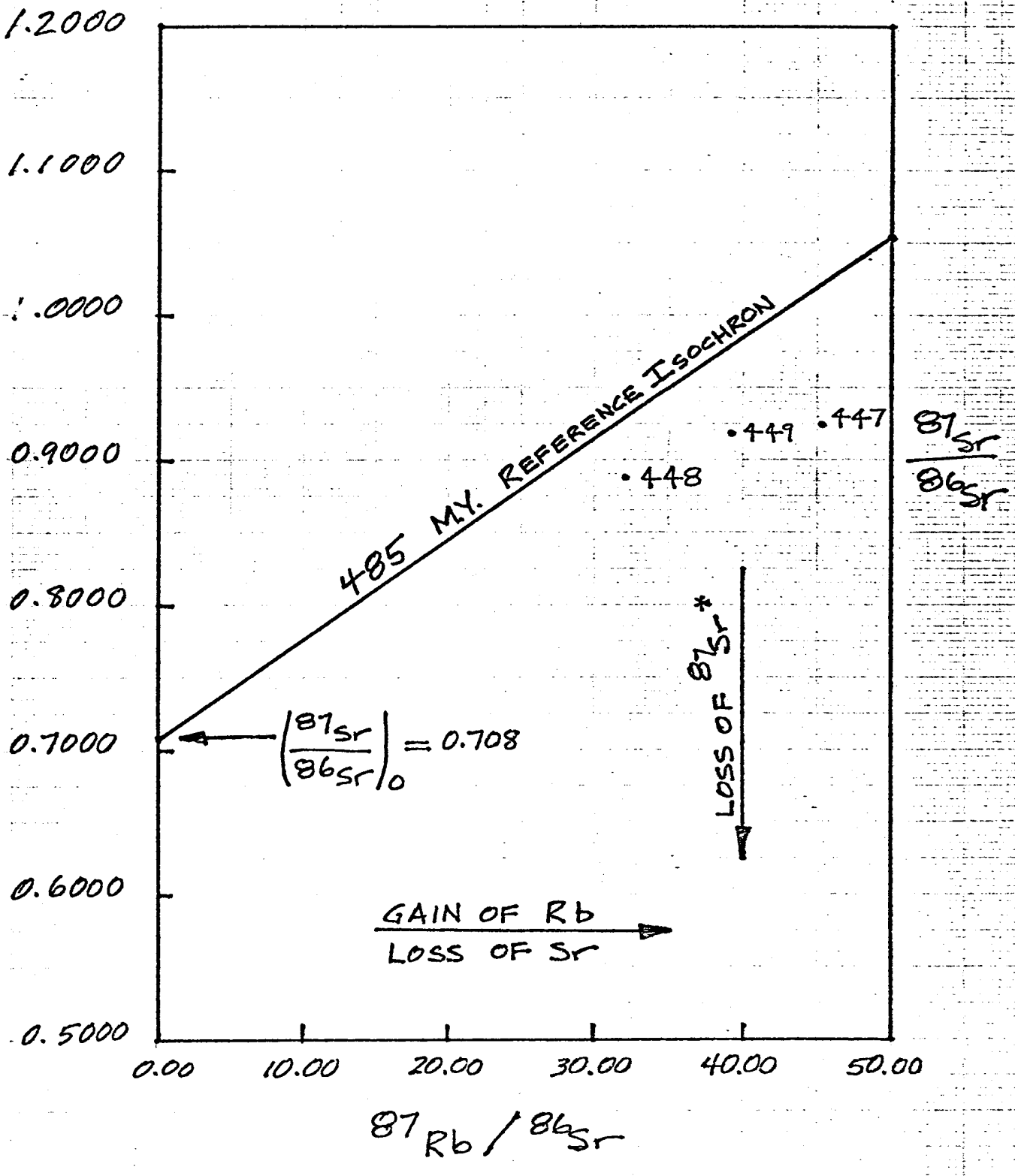

Figure 14. Rb-Sr isochron diagram. Minerals which became closed systems to Rb and Sr 485 million years ago and have stayed closed to Rb and Sr since formation should plot on the Early Ordovician reference isochron. Glauconite samples 447, 448 and 449 all plot below the reference isochron, and indicate loss of Sr or gain of Rb or both since initial closure to Rb and Sr at the time of mineral formation.

on the reference isochron. All three glauconites from this study have ages which are lower than that of the reference isochron, and therefore are plotted below it. Obviously, glauconites 447, 448 and 449 have not been closed systems as required for dating.

Addition of Rb

Because Rb behaves chemically like K, several statements may be made in regard to the addition of Rb to glauconite. Rb may be added to glauconite by cation fixation, and occurs in illite minerals by the emplacement of Rb between basal surfaces of the crystal lattice layers in the positions normally occupied by Rb or K (after Grim, 1968). Dehydration of glauconite tends to increase the fixation of Rb also (after Grim, 1968; Logvinenko et al., 1975; Velde and Odin, 1975). Glauconite could absorb Rb from any aqueous solution, including near-surface ground water, which carried Rb ions (Cooper et al., 1971).

Well-ordered micaceous minerals contain more Rb than do those micaceous minerals having less order in their structures (after Burst, 1958a). Hurley and others (1960) observed that Early Paleozoic glauconites consisted of approximately 10% expandable layers, while 'younger' glauconites commonly have up to 30% expandable layers in their crystal structures. This evidence suggests that glauconite pellets continue to

develop into better-ordered mineral grains over long periods of time. The accompanying increase in non-expandable layers at the expense of expandable layers creates basal surface area in the stacked mica sheet lattice structure to which Rb could become adsorbed. This mechanism for Rb adsorbtion over time may explain the observation made by Hurley and others (1960) that Early Paleozoic glauconites which have 10-20% fewer expandable layers than did younger glauconites used in their study yielded Rb-Sr ages that were 10-20% lower than ages obtained from muscovites in the same rocks.

More recent work suggests that this mineralogical ordering over time in glauconites involves the allogenic formation of illite layers (non-expandable) in the mixed-layered structure at the expense of the dehydrating smectite layers (expandable). Rb would be gained over time as glauconite tended to become more purely crystalline and less hydrated (Hurley et al., 1960; Hower, 1961; Owens and Sohl, 1973).

Loss of Sr

Common Sr adsorbed onto basal surfaces of the expandable lattice layers in glauconite is roughly proportional to the abundance of these layers and is easily removed by exchange (Hurley et al., 1960). Ionic exchange is facilitated by deep burial, tectonic deformation, and circulating fluids (Grim, 1968).

Cooper and others (1971) state that Sr could be absorbed from, or lost to, ground water in situ, or to any aqueous solution. Removal of Sr from glauconite reduces the calculated model date.

Increased temperature enhances the loss of Sr because hydrated layers in the crystal lattice expand as energy is added to the system, while concurrent increases in ion mobility facilitate Sr loss.

Radiogenic ^{87}Sr might be lost in light of simultaneous Rb fixation. Recall that the ionic radius of Rb (1.48 Å) is larger than that of Sr (1.13 Å). The larger ionic radius of Rb adsorbed in the glauconite grain interiors might prevent or hinder its desorbtion, while radiogenic ^{87}Sr produced from the decay of Rb could remain mobile because of its relatively smaller size. Addition of Rb to glauconite grain exteriors from aqueous solution could occur while Sr was being lost from the same grains.

CONCLUSION

Glauconites from Lower Ordovician limestone near Stenbröttet, Sweden, are not suitable for dating by the Rb-Sr method. Indeed, the mineral glauconite itself may not be suitable for dating by this method. The work of geochemists and clay mineralogists has shown that the glauconite crystal lattice tends to

become more purely crystalline over long periods of time. During this gradual recrystallization of glauconite, the amount of potassium and rubidium tends to increase, while strontium may be lost. Alteration of the initial rubidium and strontium isotope ratios, or of subsequent ratios produced by the decay of ^{87}Rb to ^{87}Sr, renders model date numbers obtained by the Rb-Sr method meaningless. Dates obtained on glauconites in this study are in agreement with with those reported from previous work. The reported dates, together with those obtained from this work fall between earliest Devonian and latest Early Mississippian time.

The temptation for speculating on the resetting of the glauconite systems by tectonic deformation associated with the Acadian Orogeny should, perhaps, be avoided, because although this event may have affected great areas of the Scandanavian Baltic Shield and Lower Paleozoic sediments, the Cambro-Silurian sequence of rocks of southern Sweden is presently nearly horizontally bedded and lacks major folding. A more convincing hypothesis for the cause of the low dates involves the circulation of fluids through the limestone host rock. Circulating fluids of either high or low temperature could have had an effect on the isotope ratios in the glauconites, and thereby adversely effect the dates obtained. Perhaps fluids

associated with the intrusion of the post-lower Silurian sill contributed to the alteration of the rubidium and strontium isotope ratios.

If circulating fluids did play a role in adding rubidium to or removing strontium from the glauconites, then it becomes interesting to note that the degree to which they were altered was apparently independent of their vertical position in the stratigraphic section. A comparison of Figure 15 with Figure 5 supports this observation. The relative amounts of rubidium and strontium in each sample is expressed as a ratio of concentrations. This is plotted against time in Figure 15. Note that the ages do not decreased up section as would normally be expected. The Rb/Sr concentration ratio appears to be independent of vertical position in the section. This observation suggests the mechanism by which the glauconites had their relative concentrations of rubidium and strontium altered varied laterally through the bedding. Perhaps this was controlled by local lateral and vertical variation in permeability.

Serious consideration of temperature increase as an isotope ratio altering mechanism is difficult, because such data for the Stenbröttet and surrounding areas is either lacking altogether, or is not readily

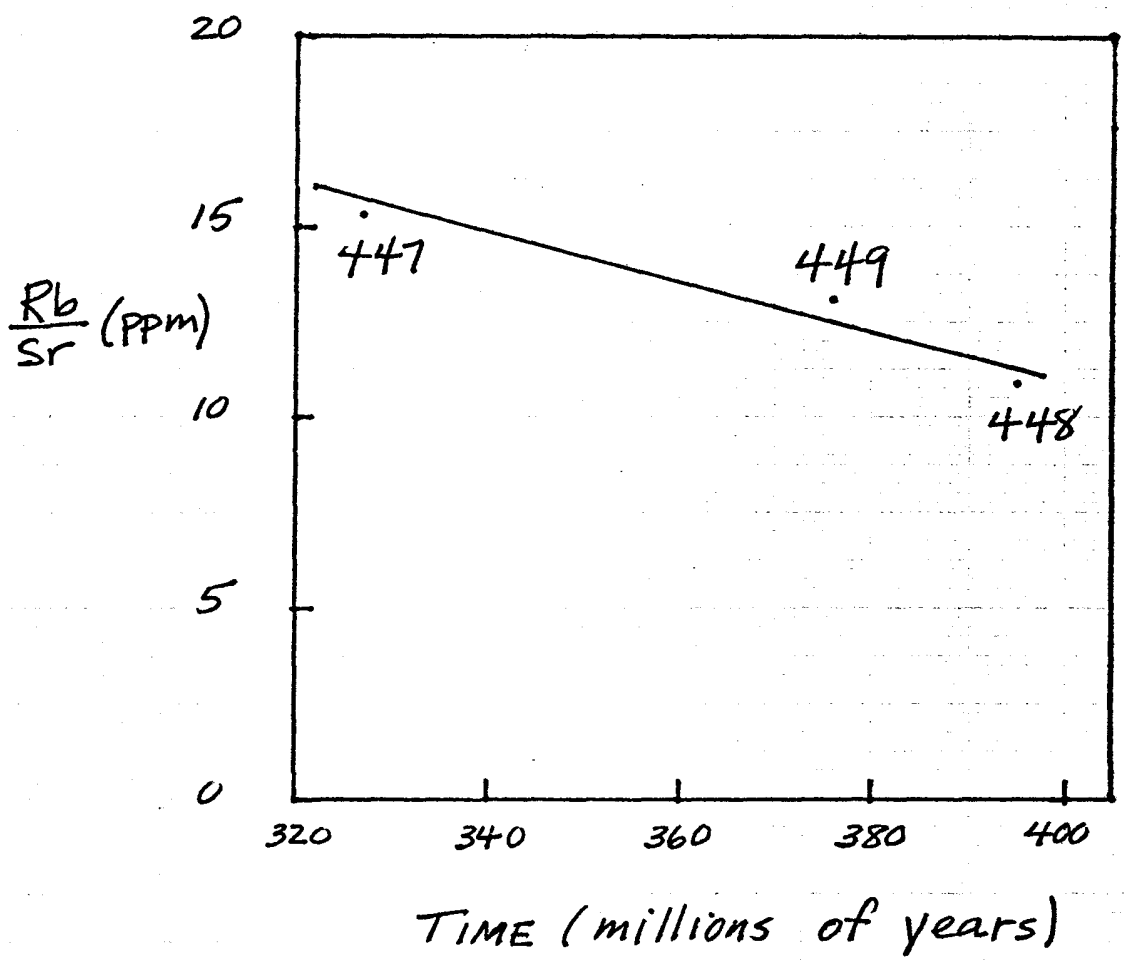

Figure 15. Rb/Sr concentration ratio of glauconites plotted against time.

avaiable. However, asphaltite blebs occur in the Cambrian alum shale 70 kilometers west of Stenbröttet, and waxy petroleum residues occur in this same unit only 10 kilometers to the west (Thorslund, 1960). This meager evidence tends to suggest the presence of either a regional source of heat at some unknown depth, or that the region was deeply buried at one time or another in the geologic past. Heat in the alum shales must have been great enough for distillation of organic material accumulations. The question of wether the glauconitic limestones from Stenbröttet were subjected to a heating event which may have affected the outcome of Rb-Sr dating of the glauconites remains unanswered.

ACKNOWLEDGEMENTS

I am indebted to my thesis advisor, Gunter Faure, for suggesting the thesis, technical assistance, numerous helpful discussions, and his patience. Dr. Stig Bergström collected the samples. Dr. Russell Utgard provided necessary support. Thanks also to Debbie Kolbe and Karen Taylor for their assistance in the lab. Special thanks to R. P. Felder for many helpful discussions.

REFERENCES CITED

Armando, G., 1973, Geochemical studies of uranium, molybdenum and vanadium in a Swedish alum shale, Stockholm Contributions in Geology, 27, 1-48.

Armstrong, R. L. and McDowall, W. G., 1974, Proposed refinement of the Phanerozoic time scale, Int. Meeting Geochron., Cosmochron. Isotope Geol., Aug. 26-31, Un. Paris, France.

Bergström, S. M., 1971, Conodant biostratigraphy of Middle and Upper Ordovician of Europe and Eastern North America, Geol. Soc. Am. Mem. 127, 83-161.

Bergström, S. M., 1973, Correlation of the late Lasnamgian Stage (Middle Ordovician) with the graptolite succession, Geol. Foren. Stockholm Forh., 95, 9-18. Stockholm.

Bergström, S. M., 1977, Early Paleozoic biostratigraphy in the Atlantic borderlands, Stratigraphic micropaleontology of Atlantic basin and borderlands, 85-110. Amsterdam.

Burst, J. F., 1958a, Mineral heterogeneity in 'glauconite' pellets, Amer. Mineral., 43, no. 5-6.

Cantanzaro, E. J., T. J. Murphy, E. L. Garner and W. R. Shields, 1969, Absolute isotopic abundance ratio and atomic weight of terrestrial rubidium, J. Res. Nat. Bur. Std. Phys. and Chem., 73A, 511-516.

Cooper, J. A., A. T. Wells, T. Nicholas, 1971, Dating of glauconite from Ngaglia Basin, Northern Territory, Australia, J. of the Geol. Soc. of Australia, 18, 97-106.

Faure, G., 1977, Principles of Isotope Geology, John Wiley & Sons, Inc., 464p.

Faure, G., R. Assereto, and E. L. Tremba, 1978, Strontium isotope composition of marine carbonates of Middle Triassic to Early Jurassic age, Lombardic Alps, Italy, Sedimentol., 25, 523-543.

Flanagan, F. T., 1973, 1972 values for the international geochemical reference samples, Geochim. et Cosmochim. Acta, 37, 1189-1201.

Grim, R. E., 1968, Clay Mineralogy, McGraw-Hill, Inc., 596p.

Harland, W. B., A. G. Smith, and B. Wilcock, eds., 1964, The Phanerozoic time scale, Quart. J. Geol. Soc. London, 1205, 485p.

Holmes, A., 1959, A revised geological time scale, Trans. Edinb. Geol. Soc., 17, 183-216.

Hower, J., 1961, Some factors concerning the nature and origin of glauconite, Amer. Mineral., 46, 313-334.

Hurlbut, C. S. Jr., 1971, Dana's Manual of Mineralogy, 18th Ed., John Wiley & Sons, Inc., 579p.

Hurley, P. M., R. F. Cormier, J. Hower, H. W. Fairbairn, and W. H. Pinson, Jr., 1960, Reliability of glauconite for age measurement by the K-Ar and Rb-Sr methods, Amer. Assoc. of Petrol. Geol. Bull., 44, 1793-1800.

Kulp, J. L., 1961, Geologic time scale, Science, 133, 1105-1114.

Lindström, M., 1971, Lower Ordovician conodants of Europe, Geol. Soc. Am. Mem. 127, 21-61, Boulder, Colorado.

Löfgren, A., 1978, Arenigian and Llanvirnian conodants from Jämtland, northern Sweden, Fossils and Strata, No. 13, 1-129, Pls. 1-16, Oslo.

Logvinenko, N. V., I. I. Volkov, and A. G. Rozanov, 1975, Genesis of the glauconite in the sediments of the Pacific Ocean, Lithol. and Min. Res., 10, 145-153.

Magnusson, N. H., P. Thorslund, F. Brozen, B. Asklund, and O. Kulling, 1960, Description to accompany the map of the Pre-Quaternary Rocks of Sweden, Sveriges Geologiska Undersökning Ser. Ba., No. 16, 69-110.

Neumann, W., and H. Huster, 1974, The half-life of ^{87}Rb measured as a difference between the isotopes ^{87}Rb and ^{85}Rb, Z. Physik, 270, 121-127.

Owens, J. P., and N. F. Sohl, 1973, Glauconite from the New Jersey-Maryland Coastal Plain: Their K-Ar ages and application in stratigraphic studies, Geol. Soc. Amer. Bull., 84, 2811-2838.

Reynolds, R. C., 1963, Matrix corrections in trace element analysis by X-ray fluorescence: Estimation of the mass absorption coefficient by Compton scattering, Amer. Mineral., 48, 1133-1143.

Thorslund, P., and V. Jaanuson, 1960, The Cambrian, Ordovician, and Silurian in Västergötland, Närke, Dalarna, and Jämtland, Central Sweden: Guide to excursions Nos A23 and C18, Edited by the Geological Survey of Sweden, 51p.

Tjernik, T. E., 1956, On the Early Ordovician of Sweden: Stratigraphy and fauna, Bull. Inst. Uppsula, 36, 109-284.

Velde, B., and G. S. Odin, 1975, Further information related to the origin of glauconite, Clays and Clay Minerals, 23, 376-381.

Herzog, L. F., W. H. Pinson, Jr., and R. F. Cormier, 1958, Sediment age determination by Rb/Sr analysis of glauconite, Amer. Assoc. Petrol. Geol. Bull., 42. No. 4, 717-733.